Size effects in the thermal conductivity of gallium oxide (β-Ga_2O_3) films grown via open-atmosphere annealing of gallium nitride (GaN)

Chester Szwejkowski,[1] Nicole Creange,[2] Kai Sun,[3] Ashutosh Giri,[1]

Brian Donovan,[1] Costel Constantin,[2,a] Patrick E. Hopkins[1,b]

1. *Department of Mechanical and Aerospace Engineering,*

University of Virginia, Charlottesville, VA, USA 22904

2. *Department of Physics and Astronomy,*

James Madison University, Harrisonburg, VA, USA 22807

3. *Department of Materials Science and Engineering,*

University of Michigan, Ann Arbor, MI, USA 48109

a) electronic mail: constacx@jmu.edu

b) electronic mail: phopkins@virginia.edu

Abstract: Gallium nitride (GaN) is a widely used semiconductor for high frequency and high power devices because of its unique electrical properties; a wide band gap, high breakdown field, and high electron mobility. However, thermal management has become a limiting factor regarding efficiency, lifetime and advancement of GaN devices and GaN-based applications. In this work, we study the thermal conductivity of beta-phase gallium oxide (β-Ga_2O_3) thin films, a component of typical gate oxides used in such devices. We use time domain thermoreflectance to measure the thermal conductivity of a variety of polycrystalline β-Ga_2O_3 films of different thicknesses grown via open atmosphere annealing of the surfaces of GaN films on sapphire substrates. We show that the effective thermal conductivity of β-Ga_2O_3 can span 1.5 orders of magnitude, increasing with an increased film thickness, which is indicative of the relatively large intrinsic thermal conductivity of bulk β-Ga_2O_3 (9.7 ± 2.5 W m^{-1} K^{-1}) and large mean free paths compared to typical gate dielectrics commonly used in GaN device contacts. By conducting TDTR measurements with different metal transducers (Al, Au, and Au with a Ti wetting layer), we attribute this variation in effective thermal conductivity to size effects in the β-Ga_2O_3 film resulting from phonon scattering at the β-Ga_2O_3/GaN interface. From our measurements, we quantify the thermal boundary conductance across the β-Ga_2O_3/GaN interface as 31.2 ± 8.1 MW m^{-2} K^{-1}, in the range of typical thermal boundary conductances previously observed non-metal/non-metal interfaces. The measured thermal properties of open atmosphere-grown β-Ga_2O_3 and its interface with GaN set the stage for thermal engineering of gate contacts in high frequency GaN-based devices.

Keywords: gallium nitride, gallium oxide, roughness, gate oxide, thermal conductivity, thermal boundary conductance, open atmosphere annealing

I. INTRODUCTION

As the characteristic times and lengths of devices decrease to scales on the order of the carrier scattering rates and mean free paths, thermal management of material boundaries can become a critical aspect of design.[1-3] In this regime, the energy transport mechanisms that are intrinsic to the materials comprising the device can contribute much less to the overall thermal resistance of the system as compared to the resistances across the individual interfaces. The efficacy of transmitting energy across these solid interfaces can be quantified via the thermal boundary conductance,[4] or Kapitza Conductance,[5] (the inverse of which is the thermal boundary resistance or Kapitza Resistance), and is the constant of proportionality that relates the heat flux to the temperature drop across this interfacial region, mathematically expressed as $h_K = q/\Delta T$, where h_K is the thermal boundary conductance, q is the thermal flux, and ΔT is the interfacial temperature drop.[4] The range of phonon-dominated thermal boundary conductances between solids at room temperature span roughly two orders of magnitude from ~5 – 500 MW m^{-2} K^{-1}, and can be strongly related to the atomic structure and chemistry around the interface.[6] To put this into perspective, this energy transport pathway can offer the equivalent thermal resistance as roughly 300 – 3.0 nm of high quality SiO_2, respectively. Given the wide spread use of thin gate oxides and additional sacrificial layers in electronic nanodevices, the addition of this thermal resistance associated with interfaces can be highly detrimental to device operation and reliability.

The need for interfacial thermal engineering has emerged as a particular bottleneck in development of high power devices.[7] Where the processor industry has hit roadblocks in maintaining Moore's Law from on chip power densities exceeding 100 W cm^{-2} (higher than a typical lab hotplate),[7] even greater power densities have been observed in radio frequency (RF) amplifier gallium nitride-based (GaN) devices.[8, 9] This increase in power density creates massive hot-spots in GaN active regions, mainly concentrated near the gate contacts, which directly leads

to underperformance and eventual failure of these devices. This thermal bottleneck therefore creates a major issue for furthering of GaN-based technologies, such as high-electron-mobility transistors (HEMTs) for high frequency devices, light emitting diodes (LEDs) for energy-efficient illumination, RADAR technologies (ship-board, airborne and ground) and high performance space satellites.

Accordingly, engineering of the thermal properties and energy transport mechanisms associated with the GaN gate contacts can elucidate thermal mitigation mechanisms to improve GaN performance by reducing Joule heating effects attributed to the thermal resistance at this junction. In a typical GaN device, such as a MOSFET, the thermal resistances associated with this junction will consist of the metal electrode, a high-dielectric constant ("high-*k*") gate oxide, the GaN channel, and the material interfaces at each of these contacts. It is well known that typical gate oxides can have very low thermal conductivities (~1 W m^{-1} K^{-1}), and can vary greatly depending on the deposition procedure.[10-12] However, the thermal properties of β-Ga_2O_3, a common gate oxide component in high frequency devices (including GaN),[13-15] are relatively unstudied. Furthermore, the effects of film thickness on the thermal properties of this oxide, corresponding thermal boundary conductances at the β-Ga_2O_3-contact interfaces, and the interfacial morphology effects on thermal transport have never been experimentally determined, which has imposed a significant roadblock in gate-contact thermal mitigation.

In response, we report on the size effects in the thermal conductivity of beta-phase gallium oxide (β-Ga_2O_3) films grown via annealing (0001) GaN surfaces in open atmosphere. We show that open atmosphere annealing of GaN surfaces can create polycrystalline, phase pure films of β-Ga_2O_3 with varying thicknesses. The duration of the GaN-anneal also leads to both surface roughness on the β-Ga_2O_3 and spiking of the β-Ga_2O_3 phase into the GaN. We measure the thermal

conductance of the β-Ga_2O_3 films and interfaces in adjunction using TDTR. From our measurements, we quantify the thermal boundary conductance across the β-Ga_2O_3/GaN interface to be in close proximity to the previously reported interface conductance inferred for SiO_2/Si interfaces, another comment gate oxide/channel interface widely found in several technologies. However, unlike typical gate oxides, we show that the effective thermal conductivity of β-Ga_2O_3 can span 1.5 orders of magnitude, increasing with an increased film thickness due to size effects from phonon scattering at the β-Ga_2O_3/GaN interface. From this analysis, we determine the intrinsic thermal conductivity of open atmosphere grown β-Ga_2O_3 is 9.7 ± 2.5 W m^{-1} K^{-1}, which is exceptionally high for typical gate oxides. This study demonstrates the promise of β-Ga_2O_3 grown via open atmosphere anneal of GaN as a potential oxide that can be used to mitigate near-gate hotspots in GaN devices.

II. GALLIUM OXIDE FABRICATION AND CHEMICAL CHARACTERIZATION

The various gallium oxide films fabricated in this study were developed from commercially available, 5 mm x 5 mm, single-side polished GaN films (3.4 μm) on sapphire substrates (430 μm) obtained from University Wafers. The GaN films have a Wurtzite crystal structure and are unintentionally n-type doped. To ensure a clean surface prior to annealing, the samples were ultrasonicated for 20 min. in acetone, 20 min. in isopropanol, 20 min. in deionized water, and then dried with inert air. Following this cleaning procedure, we annealed the samples in a tube furnace subjected to a wide variety of annealing conditions, adapted and modified from previous procedures.[16-18] Samples were annealed in 10 min. cycles between 900 – 1050 °C. This initiated not only growth of gallium oxide,[19, 20] but also varying degrees of roughness at both the surface of the gallium oxide and the gallium oxide/GaN interface, as observed previously.[21-23] The surface

roughness of the gallium oxide was determined using a combination of atomic force microscopy (AFM, Veeco DI Multimode IIIa) and mechanical profilometry. The unannealed samples (which were the smoothest), had RMS roughness values (R_q) as low as 0.5 nm while the roughest sample had R_q over 70 nm with many intermediate roughnesses in between (c.f., Fig. 1 a-h). The roughness and compositional variance on the GaN surface where growth was initiated was observed with transmission electron microscopy (TEM). The TEM images reveal that annealing not only caused growth of a rough oxide layer but also changed the compositional abruptness of the Ga_2O_3/GaN interface. Roughness and "spiking" at the interface can be seen in the TEM images presented in Fig. 1 i-n. Table 1 summarizes the Ga_2O_3 thicknesses and surface roughnesses determined from the AFM and TEM measurements.

The chemistry of the oxide layer was determined using x-ray diffraction (XRD) and x-ray photoelectron spectroscopy (XPS). In Fig. 2 a-d, we present the XRD spectra taken in the range of 2θ = 20° – 130° as a function of R_q obtained from a PANalytical X'Pert PRO MPD θ-2θ diffractometer with x-ray radiation of Cu (λ = 1.54060 Å for Cu K_α peak). The signature GaN peaks are observed at 34.39(3)° (0002), 72.69(8)° (0004), and 125.89(1)° (0006). The Sapphire peaks are observed at 41.63(1)° (0006), and 90.49(7)° (00012). The other peaks observed at 2θ = 31.16(6)°, 38.32(6)°, and 59.02(2)° correspond to crystallographic planes of (002), (202), and (113) for β-Ga_2O_3. These β-Ga_2O_3 layers are polycrystalline and form crystallites that have single crystal monoclinic structure, as determined via the AFM, TEM, and XRD. According to structure factor calculations, the Miller Indices for such monoclinic structures should obey $h+k = 2n$ with n = 1, 2, 3, 4,..∞. The d-spacing for a monoclinic crystal structure is calculated according to

$$\frac{1}{d^2} = \frac{1}{\sin^2(\beta)}\left[\frac{h^2}{a^2} + \frac{k^2\sin^2(\beta)}{b^2} + \frac{l^2}{c^2} - \frac{2hl\cos(\beta)}{ac}\right], \quad (1)$$

where *hkl* are the Miller Indices, *abc* are the unit cell lattice constants, and $\alpha\beta\gamma$ are the unit cell internal angles. Equation 1 was useful to check the Miller indices for our β-Ga_2O_3 layers by using well known values for *a*, *b*, and *c* as found in the literature.[24] With Bragg's law [i.e. $n\lambda = 2d \sin(\theta)$], we determined the *d* lattice spacings to be d_{002} = 2.867(4) Å, d_{202} = 2.346(6) Å, d_{113} =1.563(8) Å, in excellent agreement with those reported by Lv *et al.* (i.e. d_{002} = 2.82(9) Å, d_{202} = 2.34(4) Å, and d_{113} = 1.53(3) Å).[25] The O_{1s} XPS spectra in Fig. 2e are presented as a function of surface roughness for our samples with R_q = 1.0, 4.9, 9.7, and 12.7 nm. The binding energies of the examined elements were calibrated using C_{1s} peak (284.6 eV) as a reference. The binding energies for our samples were found to be 534.5 eV (R_q = 0.5 nm), 530.50 eV (R_q = 4.9 nm), 530.34 eV (R_q = 9.7 nm), and 530.15 eV (R_q = 12.7 nm). These O_{1s} spectra indicate that the as-received sample (i.e., not annealed and with 0.5 nm RMS roughness – blue curve in Fig. 2) contains a much smaller signature of oxygen compared to the annealed samples; this is consistent with typical thicknesses of native Ga_2O_3 on the GaN surface (i.e., a surface layer of 1-2 nm).[26] It is important to note that as the Ga_2O_3 layer increases in thickness, the O_{1s} shifts towards smaller binding energies, consistent with previous XPS studies showing the effect of the Ga_2O_3 on the GaN spectrum.[27]

We measured the thicknesses of the gallium oxide layer with TEM, example micrographs of which are presented in Fig. 1 i-n. The TEM analysis confirms that the increase in surface roughness measured via AFM is directly correlated to an increase in oxide layer thickness. We relate the thickness of gallium oxide to the roughness via a 3rd order polynomial fit (Fig. 3), and use this calibration for analysis of our TDTR measurements, described in more detail below.

For TDTR measurements, we electron-beam evaporate thin metal films on the various Ga_2O_3/GaN samples, using metals similar to those employed in electronic devices: 79 nm Au,

78nm Au with a 2 nm Ti wetting layer, and 89 nm Al. The film thicknesses were verified using a combination of variable angle spectroscopic ellipsometry (VASE from J.A. Woollam) and mechanical profilometry. In the case of the Al film, we were also able to confirm the film thicknesses of picosecond acoustics.[28, 29] An illustration of sample geometries studied in this work is shown in Fig. 4. Table 1 summarizes the information for each set of samples.

III. THERMAL CONDUCTIVITY MEASUREMENTS OF THE β-Ga_2O_3 FILMS

The thermal conductivities of the β-Ga_2O_3 films were measured using time domain thermoreflectance (TDTR);[30] pertinent details of TDTR and corresponding data analyses can be found in the literature.[31-33] To briefly summarize, our TDTR experiment is a pump-probe technique utilizing sub-picosecond laser pulses that are split into two paths: the pump and probe. The pump energy is absorbed by the sample and causes a change in the surface temperature of the metal film. This surface temperature decays based on the thermal properties of the materials underneath (in our case, the β-Ga_2O_3 film, the GaN film, the Al_2O_3 substrate, and the associated interfaces) and the temporal change in temperature is subsequently monitored as a function of time via the change in thermoreflectance of the probe pulse.[34-36]

In our specific experiments, we use the sub-picosecond pulses emitted from an 80 MHz Ti:Sapphire laser system as a basis of our pump-probe experiments.. The pump path is modulated at 8.8 MHz and focused onto the surface of the metal transducer layer while the thermoreflectivity of the probe path is monitored at the pump frequency with a time-delay of up to 5.5 ns after the initial heating event. The radii of the pump and probe paths are 25 μm and 6.5 μm, respectively, so the heat flow is nearly entirely dominated by cross plane conduction (normal to the interfaces). We used TDTR to characterize the thermal conductance through the β-Ga_2O_3 films and associated

interfaces in the three sets of GaN samples (each set is referring to a different metal film transducer). Each set had between six and eight samples with different surface roughnesses based on the annealing conditions, as summarized in Table 1. Finally, at least three TDTR scans were performed on each sample to ensure repeatability in our thermal measurements.

The method we use for our data analysis is described in detail in the literature.[31-33] In short, we fit a multilayer, diffusive thermal model that accounts for the periodic heating of the laser pulses to our TDTR data. The inputs to our model analysis require knowledge of the heat capacity, thermal conductivity, and thermal boundary conductance associated with each layer of the system. We used literature values for the heat capacity of GaN (Ref. [37]) and β-Ga_2O_3 (Ref. [38]) and for the heat capacities and thermal conductivities of Al (Ref. [39]) and Au (Ref. [40]). At a modulation frequency of 8.8 MHz, the thermal penetration depth in these samples is at most on the order of 2 μm. Thus, we are not sampling the sapphire layer or GaN/sapphire interface. For the as-received samples, we determined the thermal conductivity of the GaN layer using a two layer model (transducer/GaN), treating the nanometer of native oxide as an interface. This value for the thermal conductivity of the GaN layer was used for the remaining annealed samples in that set. However, because the GaN layer is so conductive, resistance to thermal transport is dominated by the GaN interface and we are relatively insensitive to the thermal conductivity of the GaN.[41] For the annealed samples we used a three layer model (transducer/ β-Ga_2O_3/GaN), fitting the thermal conductivity of the β-Ga_2O_3 layer and the thermal boundary conductance at the transducer/β-Ga_2O_3 interface. In this analysis, we assumed that the thermal boundary conductance at the β-Ga_2O_3/GaN interface was very large (i.e., we assumed that this interface offers negligible resistance), so that the measured thermal conductivities of the β-Ga_2O_3 layer from the TDTR measurements are in fact "effective" thermal conductivities that are also influenced by the

resistance at the β-Ga_2O_3/GaN interface. As discussed later, we through data analysis of the effective thermal conductivities as a function of film thickness, we resolve the intrinsic thermal conductivity of the β-Ga_2O_3 and the thermal boundary conductance across the transducer/β-Ga_2O_3 interface adapting a method used by Lee *et al.*[42] The uncertainty in our measurements factored in the repeatability of the measurements, uncertainty in film thicknesses, uncertainty in the thermal conductivity of the metal film, and uncertainty in the heat capacity of GaN and Ga_2O_3. From this, the mean uncertainty in our TDTR measurements was ~10%.

IV. RESULTS & DISCUSSION

The thermal conductivities of the gallium oxide films are plotted as a function of film thickness in Fig. 5. Our measurements follow typical thickness-dependent trends reported in the literature for thickness limited thermal conductivities of other dielectric films.[11, 42] these trends are indicative of size effects in the film that reduce the thermal conductivity due to phonon-boundary scattering. Unlike the thermal conductivities of the amorphous SiO_2 and SiN_x films, the thermal conductivity of β-Ga_2O_3 increases up to thicknesses of several hundred nanometers approaching 1 μm. This is indicative of the higher intrinsic thermal conductivity of β-Ga_2O_3 and longer phonon mean free paths compared to other typical dielectrics; this is not surprising due to the polycrystalline nature of our β-Ga_2O_3 compared to the amorphous SiO_2 and SiN_x films, which due to the lack of periodicity in their atomic structures will have intrinsically vibrational smaller mean free paths. The range in thermal conductivities of the gallium oxide layers span 1.5 orders of magnitude; 0.34 W m^{-1} K^{-1} for a film thickness of 12.5 nm up to 8.85 W m^{-1} K^{-1} for a film thickness of 895 nm. The trends are conserved for all three types of samples regarding the metal transducer. Thus, there is no appreciable dependence on the transducer.

From the data in Fig. 5, we can determine the intrinsic thermal conductivity of bulk β-Ga_2O_3 while relating the reduction in thermal conductivity due to phonon-boundary scattering to the thermal boundary conductance across the β-Ga_2O_3/GaN interface. Using the expression presented by Lee *et al.*,[42] the intrinsic thermal conductivity of β-Ga_2O_3 can be derived from our data via

$$k_m = \frac{k_i}{1+\frac{k_i}{h_K d}}, \tag{2}$$

where κ_m is the measured thermal conductivity, κ_i is the intrinsic thermal conductivity of the β-Ga_2O_3, h_K is the thermal boundary conductance, and d is the thickness of the β-Ga_2O_3. Equation 2 treats the metal/β-Ga_2O_3 thermal conductance, the thermal conductivity of the β-Ga_2O_3 film, and the β-Ga_2O_3/GaN thermal conductance as resistors in series. However, we rule out the inclusion of the resistance across the metal/β-Ga_2O_3 in calculations of Eq. 2 due to the following two reasons: i) in our TDTR analysis of the thermal conductivity of the β-Ga_2O_3, we fit both the metal/β-Ga_2O_3 thermal boundary conductance and the β-Ga_2O_3 thermal conductivity, thereby independently determining the thermal conductivity of the β-Ga_2O_3 from the metal/β-Ga_2O_3 thermal boundary conductance. During this analysis, we determine that we are inherently insensitive to the metal/β-Ga_2O_3 boundary conductance due to the relatively larger resistance of the β-Ga_2O_3 film; and ii) as shown in the inset of Fig. 5, we do not show any systematic, noticeable dependence in the measured thermal conductivity of the β-Ga_2O_3 for the samples with different metallic transducers. Since we have previously shown that the thermal boundary conductance across these metal films/native β-Ga_2O_3/GaN interfaces can vary by a factor of five depending on the metal film,[41] we conclude that this metal/β-Ga_2O_3 is not contributing to the thermal processes

measured in our TDTR experiments. Therefore, the value for thermal boundary conductance in Eq. 2 is representative of the thermal transport across the β-Ga_2O_3/GaN interface.

The inset graph shows our data and the model, adapted from Lee *et al.*,[42] represented by a black dotted line. The thermal boundary conductance is calculated to be 31.2 ± 8.1 MW m^{-2} K^{-1} and the corresponding intrinsic thermal conductivity of bulk β-Ga_2O_3 is 9.7 ± 2.5 W m^{-1} K^{-1}. This thermal conductivity is slightly lower than a previous measurement of the thermal conductivity of bulk, single crystalline β-Ga_2O_3 (13 W m^{-1} K^{-1} – black dotted line in Fig. 5).[43] Given the polycrystalline nature of our β-Ga_2O_3 films, this reduction in thermal conductivity is not surprising. Although the intrinsic thermal conductivity of our β-Ga_2O_3 is nearly an order of magnitude larger than the other typical gate insulators shown in Fig. 5 (SiO_2 and SiN_x), boundary scattering effects are pronounced enough that for typical gate oxide thicknesses, the effective thermal conductivity is reduced to similar values as these gate dielectric materials.

The opportunity for thermal benefits in GaN devices arises in manipulating the thermal boundary conductance across the β-Ga_2O_3/GaN interface. As previously mentioned, we determined h_K across this interface as 31.2 ± 8.1 MW m^{-2} K^{-1}. This is on the same order as the room temperature thermal boundary conductances reported for SiO_2/Si interfaces (h_K = 50 MW m^{-2} K^{-1})[42] and dislocation dense GaSb/GaAs interfaces grown epitaxially (h_K = 10 – 20 MW m^{-2} K^{-1}).[44] Our TEM analyses shown in Fig. 1 indicate the "imperfect" nature of the boundary between the β-Ga_2O_3 and GaN, which can lead to large reductions in thermal boundary conductance.[6] Given this relatively low conductance (large resistance) associated with this interface compared to the intrinsic thermal conduction mechanisms in bulk β-Ga_2O_3, the opportunity exists to engineer this interface and thereby increase the overall thermal conduction across a metal/β-Ga_2O_3/GaN junction.

The possibility of increasing the thermal conductance across metal/β-Ga_2O_3/GaN junctions has tremendous implications for thermal mitigation of GaN-based devices by engineering hot spots around gate regions. Beta-phase Ga_2O_3 has many of the necessary electronic characteristics to be used as a gate oxide: low density of states at the β-Ga_2O_3/GaN interface,[45] high breakdown field,[45] high dielectric constant,[45] and wide band gap.[46] Although, the β-Ga_2O_3/GaN valence and conduction band offsets are low; 1.4 eV and 0.1 eV respectively,[47] compared to 4.4 eV and 3.4 eV for SiO_2/Si[48] which could lead to increased leakage current. Furthermore, β-Ga_2O_3 is very chemically stable, even in concentrated acids,[49] which could be problematic or promotional for chemical etching procedures depending on what the end goal is. Thus, further chemical and electronic research is necessary to realize the full potential of β-Ga_2O_3 as a gate dielectric. However, this issue is outside the scope of this study; our focus is thermal characterization. Our thermal measurements of open atmosphere-grown β-Ga_2O_3 demonstrate the intrinsically larger thermal conductivity and mean free path compared to typical gate dielectrics, indicating the possibility for increase thermal spreading of heat from localized hot spots at gate/channel contacts compared to typical dielectric and passivation layers. This makes annealing of GaN to form surface layers of β-Ga_2O_3 a promising candidate for gate dielectrics and other surface passivation layers in next generation GaN devices.

V. SUMMARY

Our work reports on the size effects of the thermal conductivity of beta-phase gallium oxide (β-Ga_2O_3) thin films, a component of typical gate oxides used in such devices. We use time domain thermoreflectance to measure the thermal conductivity of a variety of polycrystalline β-Ga_2O_3 films of different thicknesses grown via open atmosphere annealing of GaN surface. We confirm

that the β-Ga_2O_3 grown from annealing the the GaN surface is phase-pure, and varies in both surface roughness and diffusion into the GaN based on annealing time. The effective thermal conductivity of β-Ga_2O_3 can span 1.5 orders of magnitude, increasing with an increased film thickness, which is indicative of the relatively large intrinsic thermal conductivity of bulk β-Ga_2O_3 (9.7 ± 2.5 W m^{-1} K^{-1}) and large mean free paths compared to typical gate dielectrics commonly used in GaN device contacts. By conducting TDTR measurement with different metal transducers (Al, Au, and Au with a Ti wetting layer), we attribute this variation in effective thermal conductivity to size effects in the β-Ga_2O_3 film resulting from phonon scattering at the β-Ga_2O_3/GaN interface. From our measurements, we quantify the thermal boundary conductance across the β-Ga_2O_3/GaN interface as 31.2 ± 8.1 MW m^{-2} K^{-1}, in the range of typical thermal boundary conductances previously observed non-metal/non-metal interfaces. The measured thermal properties of open atmosphere-grown β-Ga_2O_3 and its interface with GaN set the stage for thermal engineering of gate contacts in high frequency GaN-based devices.

ACKNOWLEDGMENTS

The material is based upon work partially supported by the Air Force Office of Scientific Research under AFOSR Award No. FA9550-14-1-0067 (Subaward No. 5010-UV-AFOSR-0067), the National Science Foundation (CBET-1339436) and the Commonwealth Research Commercialization Fund (CRCF) of Virginia.

REFERENCES

1. D. G. Cahill, P. V. Braun, G. Chen, D. R. Clarke, S. Fan, K. E. Goodson, P. Keblinski, W. P. King, G. D. Mahan, A. Majumdar, H. J. Maris, S. R. Phillpot, E. Pop and L. Shi, "Nanoscale thermal transport. II. 2003-2012," *Applied Physics Reviews* **1**, 011305 (2014).
2. D. G. Cahill, W. K. Ford, K. E. Goodson, G. D. Mahan, A. Majumdar, H. J. Maris, R. Merlin and S. R. Phillpot, "Nanoscale thermal transport," *Journal of Applied Physics* **93**, 793-818 (2003).
3. G. Chen, *Nanoscale Energy Transport and Conversion: A Parallel Treatment of Electrons, Molecules, Phonons, and Photons* (Oxford University Press, New York, 2005).
4. E. T. Swartz and R. O. Pohl, "Thermal boundary resistance," *Reviews of Modern Physics* **61**, 605-668 (1989).
5. P. L. Kapitza, "The study of heat transfer in Helium II," *Zhurnal eksperimentalnoi i teoreticheskoi fiziki* **11**, 1-31 (1941).
6. P. E. Hopkins, "Thermal transport across solid interfaces with nanoscale imperfections: Effects of roughness, disorder, dislocations, and bonding on thermal boundary conductance," *ISRN Mechanical Engineering* **2013**, 682586 (2013).
7. E. Pop, "Energy dissipation and transport in nanoscale devices," *Nano Research* **3**, 147-169 (2010).
8. A. N. Smith and J. P. Calame, "Impact of thin film thermophysical properties on thermal management of wide bandgap solid-state transistors," *International Journal of Thermophysics* **25**, 409-422 (2004).
9. R. J. Trew, "SiC and GaN transistors - Is there one winner for microwave power applications?," *Proceedings of the IEEE* **90**, 1032-1047 (2002).
10. S.-M. Lee, D. G. Cahill and T. H. Allen, "Thermal conductivity of sputtered oxide films," *Physical Review B* **52**, 253-257 (1995).
11. R. M. Costescu, A. J. Bullen, G. Matamis, K. E. O'Hara and D. G. Cahill, "Thermal conductivity and sound velocities of hydrogen-silsequioxane low-k dielectrics," *Physical Review B* **65**, 094205 (2002).
12. C. S. Gorham, J. T. Gaskins, G. N. Parsons, M. D. Losego and P. E. Hopkins, "Density dependence of the room temperature thermal conductivity of atomic layer deposition grown amorsphous alumina (Al2O3)," *Applied Physics Letters* **104**, 253107 (2014).
13. J. W. Johnson, B. Luo, F. Ren, B. P. Gila, W. Krishnamoorthy, C. R. Abernathy, S. J. Pearton, J. I. Chyi, T. E. Nee, C. M. Lee and C. C. Chuo, "Gd_2O_3/GaN metal-oxide-semiconductor field-effect transistor," *Applied Physics Letters* **77**, 3230 (2000).
14. T. D. Lin, H. C. Chiu, P. Chang, L. T. Tung, C. P. Chen, M. Hong, J. Kwo, W. Tsai and Y. C. Wang, "High-performance self-aligned inversion-channel $In_{0.53}Ga_{0.47}As$ metal-oxide-semiconductor field-effect-transistor with Al_2O_3/Ga_2O_3(Gd_2O_3) as gate dielectrics," (2008).
15. F. Ren, M. Hong, S. N. G. Chu, M. A. Marcus, M. J. Schurman, A. Baca, S. J. Pearton and C. R. Abernathy, "Effect of temperature on Ga_2O_3(Gd_2O_3)/GaN metal-oxide-semiconductor field-effect transistors," *Applied Physics Letters* **73**, 3893 (1998).
16. V. R. Reddy, M. Ravinandan, P. K. Rao and C.-J. Choi, "Effects of thermal annealing on the electrical and structural properties of Pt/Mo Schottky contacts on n-type GaN," *Journal of Materials Science: Materials in Electronics* **20**, 1018 (2009).

17. W. Cao and S. K. Dey, "Microstructure and properties of sol-gel derived $Pb(Zr_{0.3}Ti_{0.7})O_3$ thin films on GaN/sapphire for nanoelectromechanical systems," *Journal of Sol-Gel Science & Technology* **40**, 389 (2007).
18. A. Y. Polyakov, N. B. Smirnov, A. V. Govorkov, A. A. Shlensky and S. J. Pearton, "Influence of high-temperature annealing on the properties of Fe doped semi-insulating GaN structure," *Journal of Applied Physics* **95**, 5591 (2004).
19. Y. Hayashi, R. Hasunuma and K. Yamabe, "Generation and Growth of Atomic-scale Roughness at Surface and Interface of Silicon Dioxide Thermally Grown on Atomically Flat Si Surface," *Key Engineering Materials* **470**, 110 (2011).
20. H. Döscher, G. Lilienkamp, P. Iskra, M. Kazempoor and W. Daum, "Thermal stability of thin ZrO_2 films prepared by a sol-gel process on Si(001) substrates," *Journal of Vaccum Science & Technology B* **28**, C5B5 (2010).
21. Y. Dong, R. M. Feenstra and J. E. Northrup, "Oxidized GaN(0001) surfaces studied by scanning tunneling microscopy and spectroscopy and by first-principles theory," *Journal of Vaccum Science & Technology B* **24**, 2080 (2006).
22. C. J. Lu, A. V. Davydov, D. Josell and L. A. Bendersky, "Interfacial reactions of Ti/*n*-GaN contacts at elevated temperature," *Journal of Applied Physics* **925**, 245 (2003).
23. B. P. Luther, S. E. Mohney, T. N. Jackson, M. A. Khan, Q. Chen and J. W. Yang, "Investigation of the mechanism for Ohmic contact formation in Al and Ti/Al contacts to *n*-type GaN," *Applied Physics Letters* **70**, 57 (1997).
24. S. S. Kumar, E. J. Rubio, M. Noor-A-Alam, G. Martinez, S. Manandhar, V. Shutthanandan, S. Thevuthasan and C. V. Ramana, ""Structure, Morphology, and Optical Properties of Amourphous and Nanocrystalline Gallium Oxide Thin Films," *Journal of Physical Chemistry* **117**, 4194 (2013).
25. Y. Lv, L. Yu, G. Zha, D. Zheng and C. Jiang, "Application of soluble salt-assisted route to synthesis of β-Ga_2O_3 nanopowders," *Applied Physics A: Materials Science & Processing* **114**, 351 (2014).
26. X. A. Cao, S. J. Pearton, G. Dang, A. P. Zhang, F. Ren and J. M. Van Hove, "Effects of interfacial oxides on Schottky barrier contacts to *n*- and *p*-type GaN," *Applied Physics Letters* **75**, 4130 (1999).
27. K. Prabhakaran, T. G. Andersson and K. Nozawa, "Nature of native oxide on GaN surface and its reaction with Al," *Applied Physics Letters* **69**, 3212 (1996).
28. G. T. Hohensee, W.-P. Hsieh, M. D. Losego and D. G. Cahill, "Interpreting picosecond acoustics in the case of low interface stiffness," *Review of Scientific Instruments* **83**, 114902 (2012).
29. C. Thomsen, J. Strait, Z. Vardeny, H. J. Maris, J. Tauc and J. J. Hauser, "Coherent Phonon Generation and Detection by Picosecond Light Pulses," *Physical Review Letters* **53**, 989-992 (1984).
30. D. G. Cahill, K. Goodson and A. Majumdar, "Thermometry and Thermal Transport in Micro/Nanoscale Solid-State Devices and Structures," *Journal of Heat Transfer* **124**, 223 (2002).
31. P. E. Hopkins, J. R. Serrano, L. M. Phinney, S. P. Kearney, T. W. Grasser and C. T. Harris, "Criteria for cross-plane dominated thermal transport in multilayer thin film systems during modulated laser heating," *Journal of Heat Transfer* **132**, 081302 (2010).

32. A. J. Schmidt, X. Chen and G. Chen, "Pulse accumulation, radial heat conduction, and anisotropic thermal conductivity in pump-probe transient thermoreflectance," *Review of Scientific Instruments* **79**, 114902 (2008).
33. D. G. Cahill, "Analysis of heat flow in layered structures for time-domain thermoreflectance," *Review of Scientific Instruments* **75**, 5119 (2004).
34. R. Rosei, "Temperature modulation of the optical transitions involving the Fermi surface in Ag: Theory," *Physical Review B* **10**, 474 (1974).
35. R. Rosei, C. H. Culp and J. H. Weaver, "Temperature modulation of the optical transitions involving the Fermi surface in Ag: Experimental," *Physical Review B* **10**, 484 (1974).
36. R. Rosei and D. W. Lynch, "Thermomodulation spectra of Al, Au, and Cu," *Physical Review B* **5**, 3883 (1972).
37. R. Kremer, M. Cardona, E. Schmitt, J. Blumm, S. Estreicher, M. Sanati, M. Bockowski, I. Grzegory, T. Suski and A. Jezowski, "Heat capacity of α-Ga N: Isotope effects," *Physical Review B* **72**, 075209 (2005).
38. G. B. Adams Jr. and H. L. Johnston, "Low Temperature Heat Capacities of Inorganic Solids. XI. The Heat Capacity of b-Gallium Oxide from 15 to 300°K," *Journal of the American Chemical Society* **74**, 4788 (1952).
39. G. T. Furukawa, M. L. Reilly and J. S. Gallagher, "Critical Analysis of Heat—Capacity Data and Evaluation of Thermodynamic Properties of Ruthenium, Rhodium, Palladium, Iridium, and Platinum from 0 to 300K. A Survey of the Literature Data on Osmium," *Journal of Physical and Chemical Reference Data* **3**, 163-209 (1974).
40. G. T. Furukawa, W. G. Saba and M. L. Reilly, Critical analysis of the heat-capacity data of the literature and evaluation of thermodynamic properties of copper, silver, and gold from 0 to 300 K, DTIC Document, 1968.
41. B. F. Donovan, C. J. Szwejkowski, J. C. Duda, R. Cheaito, J. T. Gaskins, C.-Y. P. Yang, D. L. Medlin, C. Constantin, R. E. Jones and P. E. Hopkins, Thermal boundary conductance across metal-Gallium Nitride (GaN) interfaces from 80 - 450 K, University of Virginia, 2014.
42. S.-M. Lee and D. G. Cahill, "Heat Transport in thin dielectric films," *Journal of Applied Physics* **81**, 2590 (1997).
43. E. G. Villora, K. Shimamura, T. Ujiie and K. Aoki, "Electrical conductivity and lattice expansion of β-Ga 2 O 3 below room temperature," *Applied Physics Letters* **92**, 202118-202118-202113 (2008).
44. P. E. Hopkins, J. C. Duda, S. P. Clark, C. P. Hains, T. J. Rotter, L. M. Phinney and G. Balakrishnan, "Effect of dislocation density on thermal boundary conductance across GaSb/GaAs interfaces," *Applied Physics Letters* **98**, 161913 (2011).
45. C.-T. Lee, H.-W. Chen and H.-Y. Lee, "Metal–oxide–semiconductor devices using Ga 2 O 3 dielectrics on n-type GaN," *Applied Physics Letters* **82**, 4304-4306 (2003).
46. M. D. Losego, Interfacing Epitaxial Oxides to Gallium Nitride, North Carolina State University, 249, 2008.
47. W. Wei, Z. Qin, S. Fan, Z. Li, K. Shi, Q. Zhu and G. Zhang, "Valence band offset of b-Ga_2O_3/wurtzite GaN heterostructure measured by X-ray photoelectron spectroscopy," *Nanoscale Research Letters* **7**, 562 (2012).

48. A. Alkauskas, P. Broqvist, F. Devynck and A. Pasquarello, "Band Offsets at Semiconductor-Oxide Interfaces from Hybrid Density-Functional Calculations," *Physical Review Letters* **101**, 106802 (2008).
49. M. Passlack, E. F. Schubert, W. S. Hopson, M. Hong, N. Moriya, S. N. G. Chu, K. Konstadinidis, J. P. Mannaerts, M. L. Schnoes and G. J. Zydzik, "Ga_2O_3 films for electronic and optoelectronic applications," *Journal of Applied Physics* **77**, 686 (1995).

Table 1. Three sets of samples were fabricated regarding the metal transducer that was deposited. The roughness of the RMS surface of the samples before transducer deposition (R_q) and the thickness of the gallium oxide layer (d) are summarized.

Transducer	Au (79 nm)		Al (89 nm)		Au (78 nm) / Ti (2 nm)	
β-Ga_2O_3	R_q (nm)	d (nm)	R_q (nm)	d (nm)	R_q (nm)	d (nm)
	0.9	1.5	0.8	1.3	0.8	1.3
	6.6	18.1	4.0	9.4	6.9	19.2
	11.6	40.3	5.0	12.5	13.5	50.7
	25.9	141.9	10.8	36.3	33.8	220.4
	45.9	369.6	14.5	56.5	43.2	333.4
	60.2	585.8	19.4	89.0	77.2	895.1
			30.2	182.7		
			41.6	312.7		
			65.6	679.0		

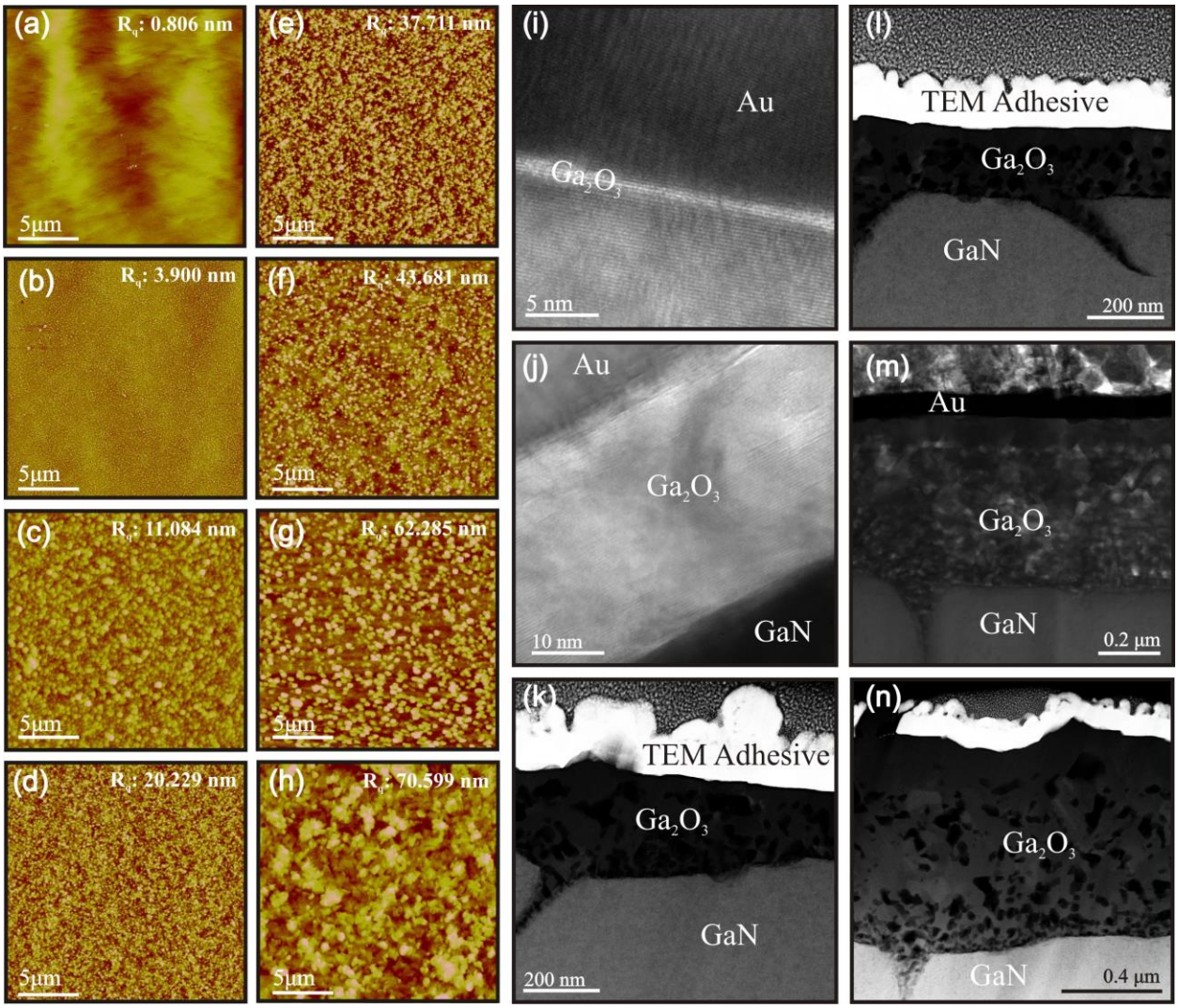

Figure 1. (a) – (h) Atomic force microscopy images of Ga_2O_3-GaN-Sapphire surfaces for R_q = 0.81 – 70.60 nm. (i) – (n) Cross-section high resolution transmission electron microscopy for sample with R_q = 0.88 – 77.22 nm.

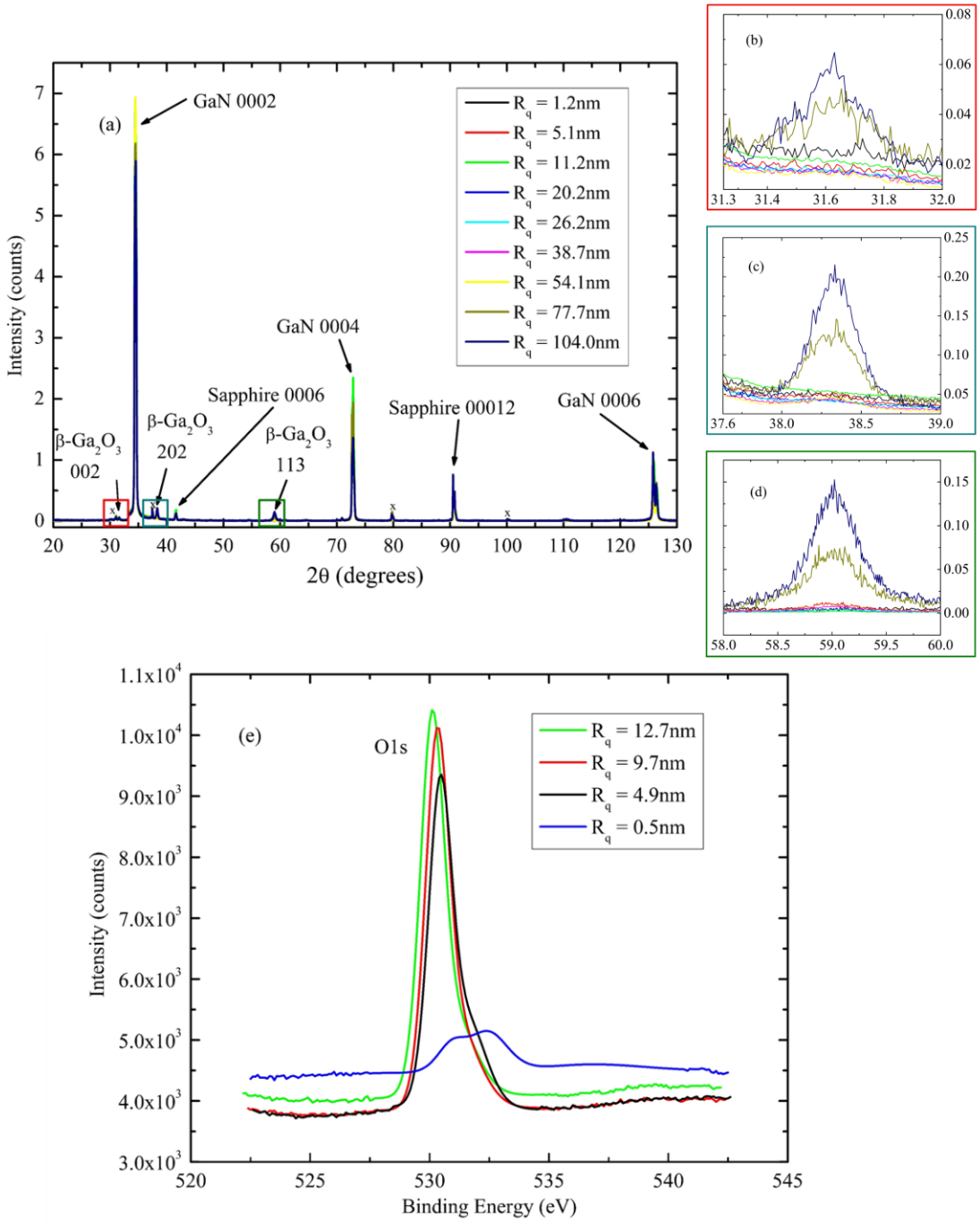

Figure 2. XRD-XPS. (a) X-ray diffraction (θ-2θ) of β-Ga_2O_3-GaN-Sapphire (0001) thin films as a function of surface roughness root mean square (R_q) for R_q = 0.9 – 104.0 nm. (b)-(d) Scaled up figures for the β-Ga_2O_3 signature peaks (i.e. 2θ = 31.6°, 38.3°, 59.0°). (e) X-ray photoemission spectroscopy for oxygen O_{1s} peak observed at ~ 530 eV.

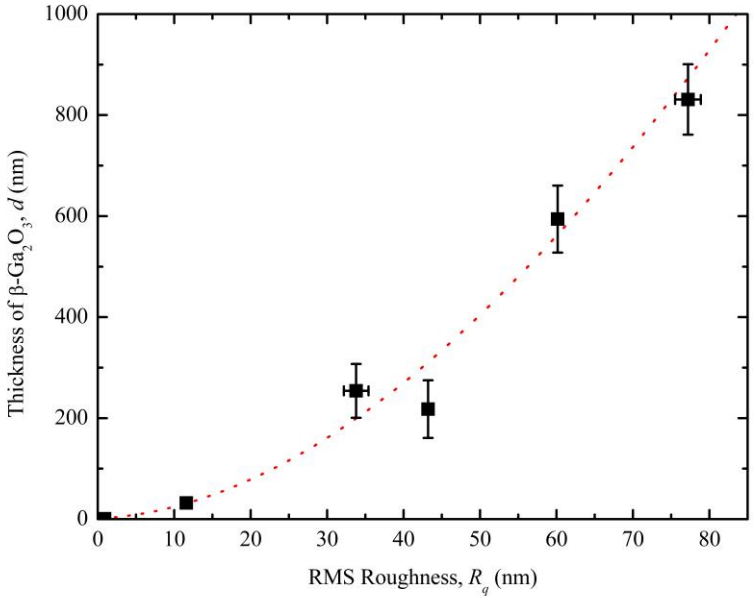

Figure 3. β-Ga_2O_3 thickness measured via TEM vs. surface roughness measured via AFM. The relationship is modeled by the red dotted line with a third order polynomial equation: $d = -0.0004(R_q)^3 + 0.1667(R_q)^2 + 0.6869(R_q) + 1.5$. This was found to be a statistically sound correlation ($R^2 = 0.975$, $t = 12.6$, $t_{\alpha=0.005} = 4.60$).

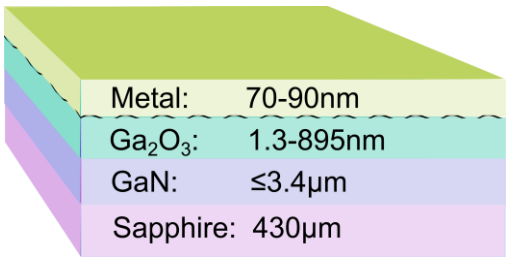

Figure 4. Illustration of sample geometries studied in this work. The fabrication of our samples includes two stages: the gallium oxide growth and then the metal film deposition. Starting with the commercially available GaN on sapphire, the oxide was grown via open atmosphere annealing for ten minute cycles at temperatures between 900 – 1050°C; longer anneals increased the roughness at the oxide surface (indicated by the textured line above the oxide layer). Various metal films were then electron-beam evaporated on top including aluminum, gold, and gold with a titanium adhesion layer.

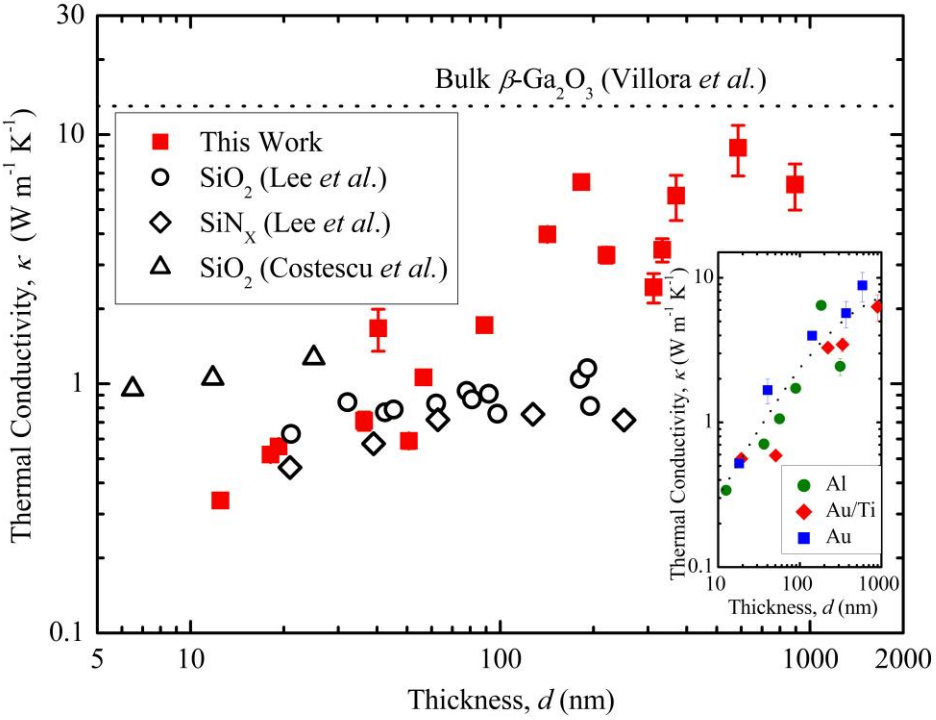

Figure 5. Measured Thermal conductivity as a function of film thickness for our β-Ga_2O_3 films compared to other thin film dielectrics. The thermal conductivity of gallium oxide (filled squares) increases with increased film thickness and approaches the previously report bulk thermal conductivity (dotted line).[43] This follows the same trend as other dielectric films reported by Lee *et al.*[42] (open cirles: SiO_2; diamonds: SiN_x) and Costescu *et al*.[11] (open triangles: SiO_2) and is attributed to boundary scattering. (inset) Measured thermal conductivity vs. thickness of β-Ga_2O_3 films with the different metal transducers used (filled circles: aluminum; filled diamonds: gold with titanium wetting layer; filled squares: gold), suggesting that the thermal resistance at the transducer/β-Ga_2O_3 is negligible; from this, we conclude that the primary mechanism driving the size effects in the measured thermal conductivities of these films is the thermal resistance associated with the β-Ga_2O_3/GaN interface The black dashed line is the model used to resolve the thermal boundary conductance across the β-Ga_2O_3/GaN interface, adapted from Lee *et al.*[42]